Magnitude Scaling of Regional-phase Amplitudes from the DPRK Announced Nuclear Tests

Sheila Peacock, David Bowers and Neil Selby
AWE Blacknest (sheila@blacknest.gov.uk)

May 2020

Document reference: AWE/DFS/20/B/527

Summary

At regional distances ($<\sim$1700 km) the phases P_n, P_g and L_g are generally the most prominent arrivals from a crustal seismic source. Amplitude ratios of P_n or P_g to L_g have been investigated by several authors (e.g. Hartse *et al.* 1997) as earthquake/explosion discriminators. Theory and observation show that explosions generate shear-wave energy less efficiently than earthquakes, hence the amplitude ratio of P_n and P_g to L_g is expected to be higher for explosions, especially at frequencies above $\sim$2 Hz. Walter *et al.* (2018) showed that amplitude ratios P_g/L_g and P_n/L_g at 2-4 Hz were clear discriminants between the six announced nuclear tests of the Democratic People's Republic of Korea (DPRK) and a population of earthquakes. We investigate regional-phase amplitudes for stations MDJ (distance $\sim$375 km), USRK ($\sim$405 km), and BJT ($\sim$1103 km) from the explosions. Walter *et al.* found a weak dependence of P_g/L_g in the 2-4 Hz band at MDJ on the magnitude M_w of the explosion. We find no clear dependence at any of the three stations. We also explore the regional amplitude behaviour at a range of frequencies, and dependence on different magnitude measures, such as network body-wave and surface-wave magnitudes.

S-wave production by underground nuclear explosion

This is a postulated 1- or 2-D source explanation of possible contributing phenomena, combined with 3-D path scattering phenomena. The underground explosion source combines (a) an explosive monopole source, (b) damage-zone and free-surface effects represented by a vertical dipole source (compensated linear vector dipole - CLVD) (Patton & Taylor, 1995, 2008, 2011), and (c) tectonic stress release, represented by a double couple. (b) and (c) can produce *S* waves directly. The free surface and internal interfaces can create *S* waves by mode conversion. Scattering of *S* and surface waves in turn produces the L_g phase.

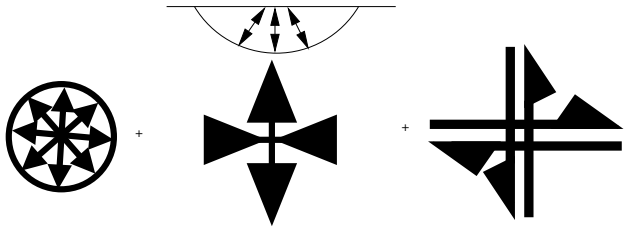

Simplified sketch of seismic sources from an underground explosion, after Patton & Taylor 2011.

L_g magnitudes and source mechanism

The amount of L_g energy relative to P_n and P_g energy may indicate contributions of topography, damage and tectonic release to S-wave generation (e.g. Patton & Taylor 1995). The depth of burial and strength of the overburden, as well as the explosion size, affect the contribution of the tensile-failure component.
A graph of L_g amplitude against magnitude measured on other phases, particularly teleseismic m_b, should show a gradient different from one if these factors are important.

Stations used in this study

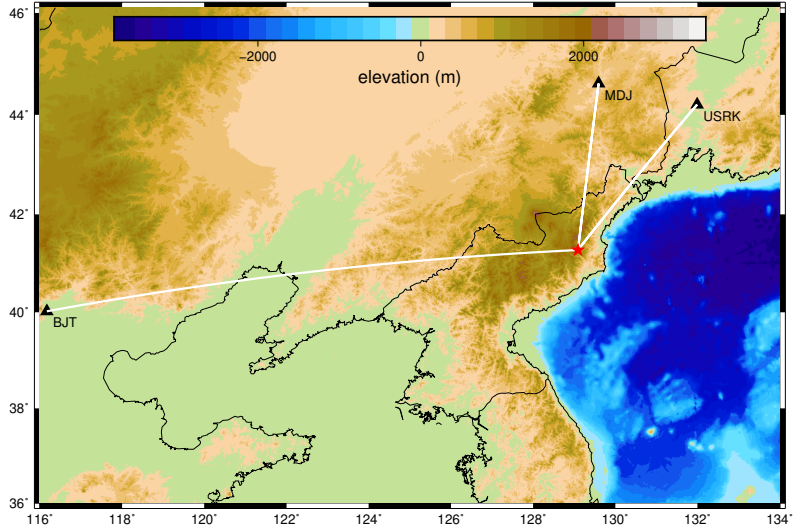

Stations (triangles) with raypaths from the test site (star) that do not cross the continental shelf were chosen, to avoid excessive scattering of the regional phases. USRK in Russia (405 km from the test site) is a CTBTO International Monitoring System station; MDJ (375 km) and BJT (1103 km) belong to the Chinese national network.

Regional Phases received at MDJ

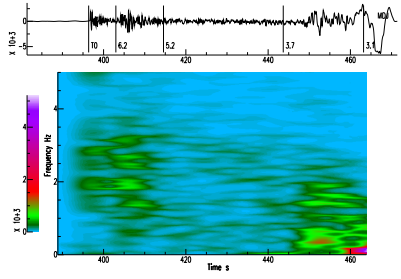

← DPRK2

The spectrogram of the signal from the second announced test (DPRK2, 2009, m_b 4.54) (upper image) shows that the P_n first arrival (T0) and the P_g phase (speed 6.2-5.2 km/s as shown) have frequency 1-3.5 Hz while the L_g (speed 3.7-3.1 km/s as shown) has frequency 0.5-2 Hz. The high-amplitude arrival on the extreme right is R_g with frequency $<$ 0.5 Hz. DPRK6 (2017, m_b 6.10) (lower image) shows lower dominant frequencies ($<$ 2 Hz) of P_n and P_g and smaller amplitudes relative to L_g and R_g. Times are in s, amplitudes in nm and square-root scaling has been applied to amplitudes in the spectrograms.

← DPRK6

Regional Phases received at USRK

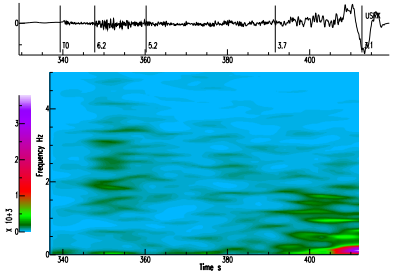

← DPRK2

The spectrograms of the signal at USRK from DPRK2, upper image) and DPRK6 (lower image) show the same features as at MDJ, including enhanced low frequencies relative to frequencies above 2 Hz from DPRK6. Y-axis scale ticks on seismogram are at 2.5×10^3 nm intervals for DPRK2 and 10^5 nm intervals for DPRK6.

← DPRK6

Regional Phases received at BJT

DPRK2 →

The spectrograms at BJT of arrivals from DPRK2 (upper) and DPRK6 (lower) do not show a clear P_g onset (speed 6.8-5.2 km/s). P_n and L_g show enhanced low frequencies from DPRK6. The greater distance to BJT (1103 km) causes lower signal-to-noise ratio for noise at $<$0.5 Hz, which dominates the seismogram for DPRK2 P_n and P_g (upper left) and appears in red along the bottom of the spectrograms. Y-axis scale ticks are at intervals of 5x10^2 nm for DPRK6 P_g and DPRK2 L_g, and 10^4 nm for DPRK6 L_g.

DPRK6 →

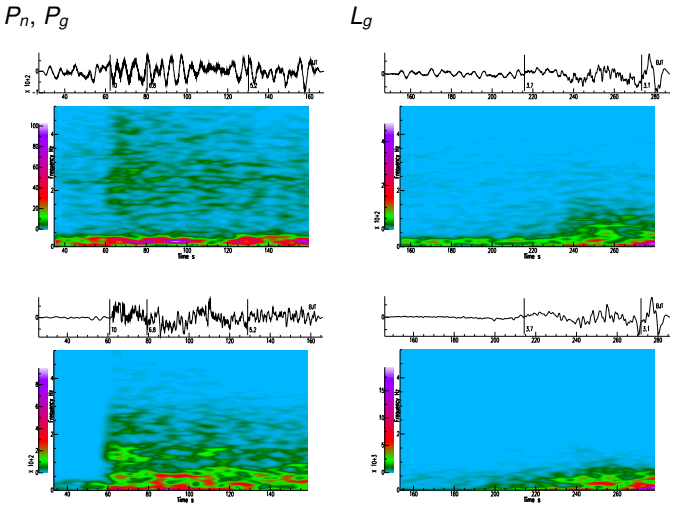

L_g amplitude and $m_b(L_g)$ vs. m_b

Log RMS amplitude of L_g arrivals and $m_b(L_g)$ (Nuttli 1973; Patton 1988) are plotted against maximum-likelihood m_b. Solid line - RMS from vertical component; dotted line - RMS from sum of squares of three components.

The quality factor Q_0 at 1 Hz and the Q-frequency dependence factor ζ used to derive $m_b(L_g)$ from L_g RMS amplitudes are unknown for paths to USRK or BJT. The values for MDJ, Q_0 = 317 and ζ=0.343 (Chun & Henderson 2009 "Q_{EX}") aren't right for USRK or BJT because there is still distance dependence.

One-to-one correspondence with m_b is good apart from DPRK6, which may be affected by lack of high frequencies from source.

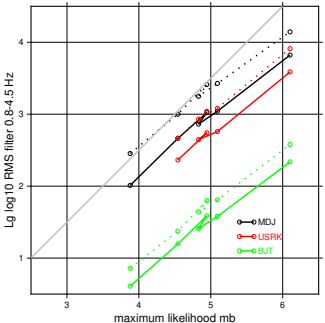

Log RMS amplitude of L_g (filtered 0.8-4.5 Hz) vs. m_b (Selby *et al.* 2018). Grey line has gradient 1 for comparison.

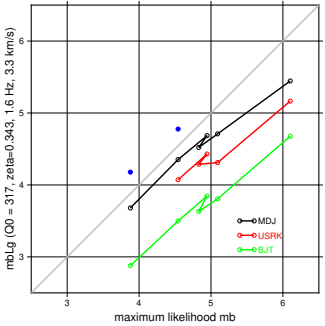

$m_b(L_g)$ vs. m_b. Grey line shows 1-to-1; blue dots: Chun *et al.* 2011 MDJ $m_b(L_g)$ for DPRK1 and 2.

Frequency dependence

When the L_g arrival is filtered at 2-4 Hz the amplitude from DPRK6 is depleted more relative to amplitudes from the other five tests, compared with the 0.8-4.5-Hz filter.

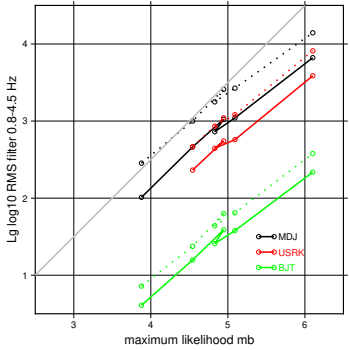

Log 0.8-4.5-Hz filtered L_g amplitude vs. m_b. Grey line has gradient 1 for comparison.

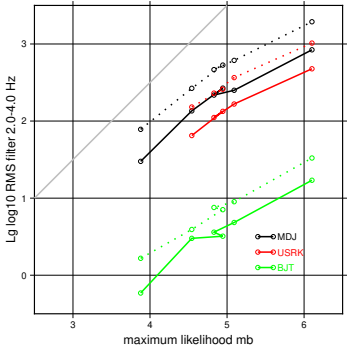

Log 2.0-4.0-Hz filtered L_g amplitude vs. m_b. Grey line has gradient 1.

m_b-L_g amplitude compared with m_b-M_S screening

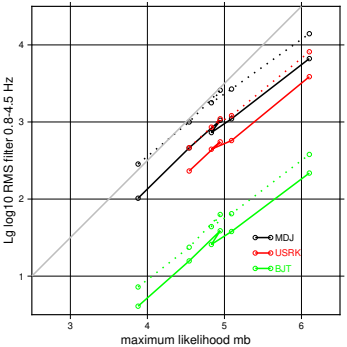

Log L_g RMS amplitude (0.8-4.5-Hz filter) vs. m_b at stations MDJ, USRK and BJT for the six DPRK tests.

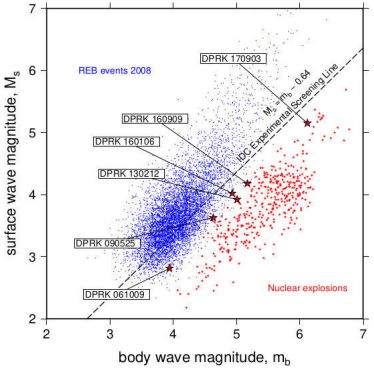

M_s vs m_b for underground explosions and earthquakes including the six DPRK tests (stars) (N. Selby, unpublished).

In the $M_S - m_b$ plot the six DPRK tests lie on a straight line, unlike the plot of L_g amplitude vs. m_b. High frequency depletion of DPRK6 reduces the amplitude of L_g at > 0.5 Hz but not the Rayleigh waves at $\sim$0.05 Hz measured for M_S.

L_g amplitude at 0.8-4.5 Hz vs. m_b and M_s

M_s values are from Selby *et al.* (2018) from 17 stations including MDJ, USRK and BJT, except for DPRK1, for which 6 stations were used including MDJ and BJT but not USRK.

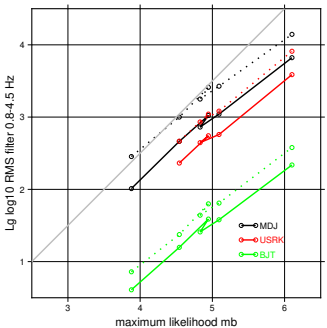

vs. m_b.

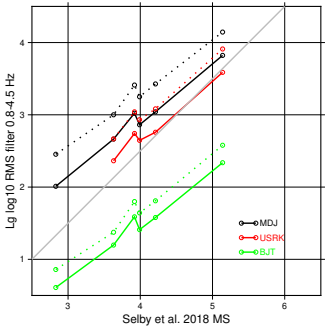

vs. M_S.

M_S is lower than m_b by average 0.94 units, so the points have moved leftwards. Against M_S the L_g amplitudes follow a straighter line than against m_b but its slope is shallower than 1. This is consistent with depletion of energy in the 0.8-4.5-Hz frequency band relative to the M_S frequency of $\sim$0.05 Hz as magnitude rises.

P_g amplitude vs. m_b and M_S

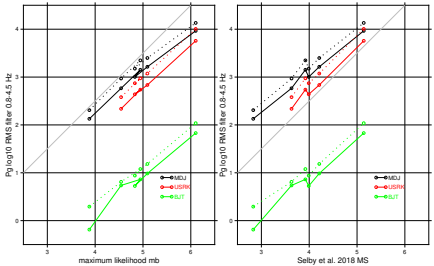

Log 0.8-4.5 Hz filtered P_g amplitude vs. m_b and M_S. Grey line has gradient 1.

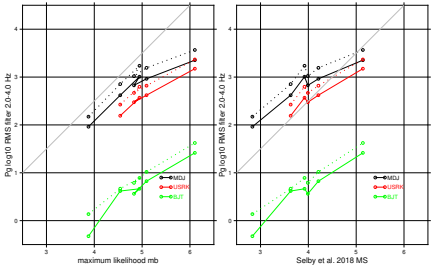

Log 2.0-4.0 Hz filtered P_g amplitude vs. m_b and M_S. Grey line has gradient 1.

The plots of P_g log amplitude vs. m_b and M_S are similar to that for L_g, and again the 2-4 Hz filter removes more of DPRK6 P_g energy relative to the other shots.

P_n amplitude vs. m_b and M_S

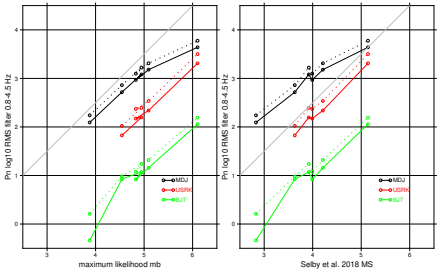

Log 0.8-4.5 Hz filtered P_n amplitude vs. m_b and M_S (Selby et al. 2018). Grey line has gradient 1.

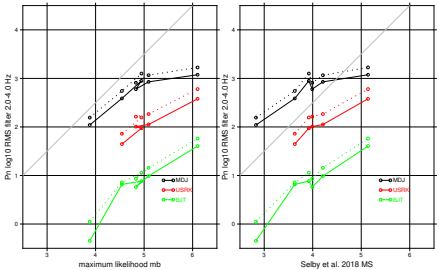

Log 2.0-4.0 Hz filtered P_n amplitude vs. m_b and M_S. Grey line has gradient 1.

The plot of P_n log amplitude vs. m_b has two obvious differences from the P_g graph: P_n from DPRK6 at MDJ is depleted relative to the other shots in both wide and narrow frequency bands; and USRK P_n amplitude from all shots is depleted relative to MDJ.

Amplitude ratios P_g/L_g and P_n/L_g

Walter *et al.* (2018) found a slight upward trend of the ratio P_g/L_g vs. magnitude "M_w" for frequency band 2-4 Hz for MDJ, but only for the RMS average of amplitudes of the three components, not for the vertical component.

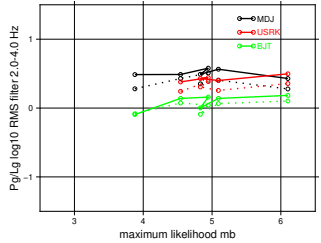

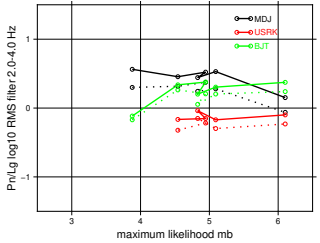

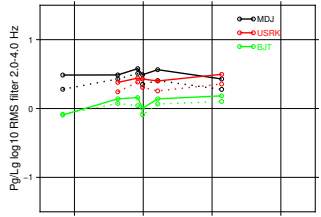

Selby et al. 2018 MS

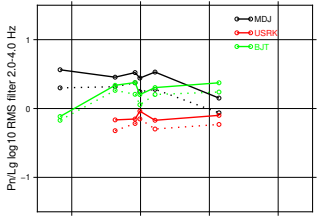

Selby et al. 2018 MS

At 2-4 Hz we see no obvious trend of P_g/L_g vs. magnitude m_b or M_S at any of the three stations, whether the vertical component (solid line) or the RMS of the three components (dotted line) is used.

Discussion, Conclusions

- For DPRK1-5, P_n, P_g and L_g energy between 0.8 and 4.5 Hz has a gradient of $\sim$unity against m_b. For L_g this suggests that the non-explosive components of the total explosion source (decompaction and tectonic release) scale linearly with the size of the explosion.
- P_n, P_g and L_g energy, particularly above 2 Hz, is depleted relative to $\sim$0.05-Hz surface-wave energy from DPRK6 compared with the other shots. In what way is this due to the size of the explosion?
  - The larger the explosion, the larger the explosive component relative to tectonic release and decompression dipole (Patton & Taylor 2008) because of more extensive damage caused by slapdown (Stevens & O'Brien (2018) conclude that large near-surface deformations, $\sim$2-4 m, could have occurred) ; or
  - The depth of burial was greater, possibly chosen according to the anticipated yield, reducing the decompression dipole;
- We see no trend in the amplitude ratio P_g/L_g vs. magnitude for the six tests at any of the three stations, for frequency ranges 0.8-4.5 Hz or 2-4 Hz.

Thank you and References

Acknowledgements to IRIS http://www.iris.edu (MDJ, BJT) and the CTBTO International Data Centre, Vienna (http://www.ctbto.org) (USRK) as the sources of the seismic data; GMT (Wessell *et al.* 2013) and SAC (Goldstein *et al.* 2003) for software for the graphing and processing respectively.

References

Chun, K.-Y., & Henderson, G.A., 2009, Bull. Seism. Soc. Am., 99, 3030-3038.
Chun., K.-Y., Wu, Y., & Henderson, G. A., 2011, Bull. Seism. Soc. Am., 101, 1315-1329.
Goldstein, P. D., *et al.*, 2003, in "The IASPEI International Handbook of Earthquake and Engineering Seismology", ed. Lee, W. H. K., *et al.*, Academic Press, London.
Hartse, H. E., *et al.*, 1997, Bull. Seism. Soc. Am., 87, p551-568.
Nuttli, O., 1973, J. Geophys. Res., 78, 876-885.
Patton, H. J.,1988, Bull. Seism. Soc. Am., 78, 1759-1772.
Patton, H. J., & Taylor, S. R., 1995, Bull. Seism. Soc. Am., 85, 220-236.
Patton, H. J., & Taylor, S. R., 2008, Geophys. Res. Lett., 35, DOI:10.1029/2008GL034211
Patton, H. J., & Taylor, S. R., 2011, J. Geophys. Res., 116, DOI:10.1029:2010JB007937.
Selby, N., *et al.*, 2018, UKNDC Technical Report 8, AWE.
Stevens, J. L., & O'Brien, M., 2018, Seism. Res. Lett. 89, 2068-2077, DOI:10.1785/0220180099
Walter, W. R., *et al.*, 2018, Seism. Res. Lett., 89, 2131-2138, DOI:10.1785/0220180128
Wessell., P., *et al.*, 2013, EOS Trans. AGU, 94, 409-410.